β Limit Disruptions in Tokamaks

Robert G. Kleva and Parvez N. Guzdar
Institute for Plasma Research, University of Maryland, College Park, Maryland 20742-3511
(Received 10 July 1997)

Nonlinear magnetohydrodynamic simulations that reproduce and elucidate the salient features observed during β limit disruptions in tokamaks are presented. Confinement is destroyed by fingers of hot plasma that jet out from the center of the discharge to the edge, while fingers of cold edge plasma are injected into the center. The loss of confinement is extremely rapid; confinement is destroyed in just a few tens of microseconds, in agreement with experimental observations. The magnetic field is virtually unchanged during the rapid loss of energy confinement, which is also in agreement with experiment. [S0031-9007(98)05730-5]

PACS numbers: 52.55.Fa, 52.35.Py, 52.65.Kj

The fusion of light nuclei in a hot plasma confined by magnetic fields is a potentially unlimited source of energy. The tokamak is a magnetic confinement device in which the hot plasma is confined by magnetic field lines that spiral around in a torus. An important parameter characterizing tokamak operation is the ratio β of the plasma pressure to the pressure in the confining magnetic field. To increase the fusion reaction rate while reducing the cost of the confining magnets, operation at large β is very desirable. However, the amount of plasma energy that can be stably confined in tokamak discharges is limited by disruptions. When a threshold in the plasma β is exceeded during a tokamak discharge, then there is a sudden, unexplained, very rapid loss of energy. The time scale over which the energy is lost is very short, on the order of a few tens of microseconds [1], much shorter than an electron-ion collision time. This loss of energy occurs with little or no warning [1]; in many cases there is no precursor magnetohydrodynamic (MHD) activity. In contrast to disruptions at high density, there is no negative voltage spike associated with the thermal quench in high β disruptions and there is no evidence of flux reconnection [1]. Thus, while thermal confinement is rapidly lost, the magnetic field remains virtually unchanged.

In this Letter we present numerical simulations that reproduce the salient features of the thermal quench in high β disruptions in tokamaks, and which elucidate the physics underlying the disruption. These simulations are based on the nonlinear resistive MHD equations for the pressure P, the magnetic field $\mathbf{B}$, the mass velocity $\mathbf{V}$, and the mass density ρ_m, including the effects of a plasma resistivity η in Ohm's law and a viscosity μ in the momentum equation [2]:

$$\partial \mathbf{B}/\partial t = \nabla \times (\mathbf{V} \times \mathbf{B}) + \eta \nabla^2 \mathbf{B}\,, \tag{1}$$

$$\partial \mathbf{U}/\partial t + \nabla \cdot (\mathbf{V}\mathbf{U}) = \mathbf{J} \times \mathbf{B} - \nabla P + \mu \nabla^2 \mathbf{U}\,, \tag{2}$$

$$\partial P/\partial t + \nabla \cdot (\mathbf{V}P) = 0\,, \tag{3}$$

$$\partial \rho_m/\partial t + \nabla \cdot \mathbf{U} = 0\,, \tag{4}$$

where the momentum density $\mathbf{U} = \rho_m \mathbf{V}$. The MHD equations are solved in toroidal geometry (R, ϕ, z), where R is the major radial coordinate of the torus, ϕ is the toroidal angle, and z is the vertical distance along the axis of the torus, with a square conducting wall of half-width a in the poloidal plane. The equations are given in normalized units [2] in which the time t is normalized to the Alfvén time $\tau_A \equiv a/v_A$, with v_A the Alfvén velocity, and the resistivity $\eta = S^{-1}$, where the Lundquist number $S \equiv \tau_r/\tau_A$ is the ratio of the resistive diffusion time τ_r to the Alfvén time. Axisymmetric equilibria, independent of the toroidal angle ϕ, are obtained dynamically [2] by evolution of the two-dimensional MHD equations [(1)–(4)] in the poloidal plane (R, z), with $\eta = 0$ but with nonzero μ, until the forces balance: $\mathbf{J} \times \mathbf{B} = \nabla P$. The initial magnetic field is given by $\mathbf{B} = \nabla\psi \times \hat{\phi}/R + B_{\phi 0}(R_0/R)\hat{\phi}$, where ψ is the flux, R_0 is the major radius of the torus, $B_{\phi 0}$ is the initial magnitude of the toroidal magnetic field at $R = R_0$, and $\hat{\phi}$ is a unit vector. The initial flux function $\psi = Cf(x)f(z)$, where $f(x) = \int_{-a}^{x} y\,dy/(1 + \alpha y^{2l})^{1/l}$, $x = R - R_0$, $\alpha = [(\bar{q}/q_0)^l - 1]a^{-2l}$, $C = B_{\phi 0}/[q_0 f(0)]$, q_0 is the value of the safety factor q at the magnetic axis, and $\bar{q}$ and l are parameters which describe the safety factor profile. The shapes of the initial flux surfaces adjust dynamically until force balance is obtained in equilibrium. The shape of the safety factor profile q is characterized by the parameter l; as l increases from unity, the q profile becomes flatter around the magnetic axis. The equilibrium pressure is given by a flux function $P(\psi) = P_0\{1 - [1 - (\psi/\psi_0)^3]^2\}$, where $\psi = \psi_0$ at the magnetic axis, and $\psi = 0$ at the wall. This pressure profile is flat around the magnetic axis with $dP/d\psi = 0$ at the axis, and is relatively broad. The ratio of the pressure P_0 at the magnetic axis to the square of the mean poloidal magnetic field is denoted by β_{pol} [2]. The equilibrium mass density is uniform in space.

We consider a high β toroidal equilibrium with $\beta_{\mathrm{pol}} = 1$ in a torus with aspect ratio $A \equiv R_0/a = 3$. The safety factor at the magnetic axis $q_0 = 1.1$ in this equilibrium, $\bar{q} = 4.5$, and $l = 2$. The nonlinear, three-dimensional time evolution of a perturbation applied to this equilibrium, in a plasma with $\eta = \mu = 3 \times 10^{-4}$, is shown in Fig. 1. This figure is a plot of the pressure in the poloidal plane (R, z) at $\phi = 0$ at four different times during the evolution. The lightly shaded areas near the center of the poloidal cross section in Fig. 1(a) are the regions of hotter, high pressure plasma, while the colder, low pressure plasma is located in the darker regions. The equilibrium is unstable to ballooning modes that grow on the pressure gradient on the large major radius (bad magnetic curvature) side of the magnetic axis. At $t = 0$ the perturbation is small, but it grows rapidly. By $t = 80\tau_A$ [Fig. 1(b)] fingers of hot plasma from the center of the column are jetting outwards on the large major radius side of the discharge, while the cold edge plasma is injected in towards the center. In the nonlinear phase the instability leads to the creation of steeper gradients in the pressure that accelerate the growth of the fingers. This process continues in time without saturating, and by $t = 180\tau_A$ [Fig. 1(d)] confinement is destroyed as the hot plasma jetting from the center nears the wall at large R, while the cold plasma that was formerly at the edge reaches into the center of the column.

The results in Fig. 1 demonstrate that thermal confinement is rapidly lost within 200 Alfvén times. To relate this time scale to observed disruption times in the Tokamak Fusion Test Reactor (TFTR) [1] (major radius $R_0 = 2.6$ m, minor radius $a = 80$ cm, temperature $T = 8$ keV, density $n = 5 \times 10^{13}$ cm^{-3}, toroidal magnetic field $B_\phi = 40$ kG), one Alfvén time in TFTR is approximately equal to 0.1 μsec. Thus, in the simulation shown in Fig. 1 the thermal energy is lost in less than 20 μsec, a result that is consistent with the time scale for rapid energy loss observed during high β disruptions [1].

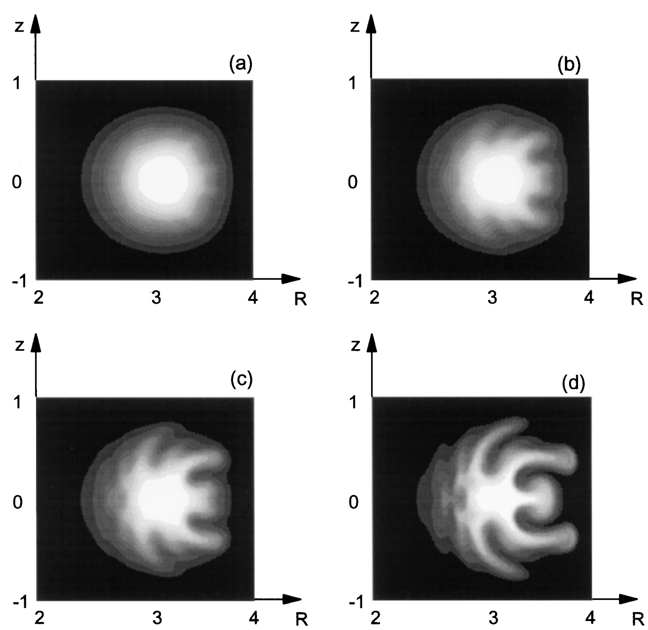

FIG. 1. Temporal evolution of the pressure in the poloidal plane (R, z) at $\phi = 0$ for a plasma with $\beta_{pol} = 1.0$ and $\eta = \mu = 3 \times 10^{-4}$, at $t/\tau_A = 0$ (a), 80 (b), 120 (c), and 180 (d).

The evolution of the magnetic field during this period of rapid loss of thermal confinement is shown in Figs. 2(a) and 2(b). Figure 2(a) is a plot of the magnitude of the poloidal magnetic field at $t = 0$; the poloidal field is largest in the lighter areas. A corresponding plot of the poloidal field at $t = 180\tau_A$, when thermal confinement is destroyed, is shown in Fig. 2(b). These two plots of the poloidal magnetic field are nearly identical, and they demonstrate that the magnetic field remains virtually unchanged even as thermal confinement is rapidly destroyed, in agreement with experimental observations of the thermal quench during β limit disruptions [1].

The flow responsible for the rapid loss of confinement is shown in Fig. 2(c). This figure is a plot of the momentum $U_R = \rho_m V_R$ in the direction of the major radius at $t = 180\tau_A$. The more lightly shaded areas are regions of outward flow in R, while the flow is inward in R in the darker areas. The flow speed increases continuously in time as confinement is destroyed. In the nonlinear phase the convection cells deepen and become extended as they reach all the way from the magnetic axis at the center of the column out to the wall.

In order to obtain adequate numerical resolution, the magnitude of η and μ used in the nonlinear simulations is much larger than that in high β tokamaks where the peak value of $S \sim 10^9$. The effect of varying η and μ on the linear MHD stability of the $\beta_{\rm pol} = 1$ equilibrium is shown in Fig. 3. This figure is a spectral plot of the linear growth rate γ of modes that vary as $e^{-in\phi}$, with toroidal mode number n, for three different values of $\eta = \mu$. When $\eta = \mu = 3 \times 10^{-4}$, the growth rate

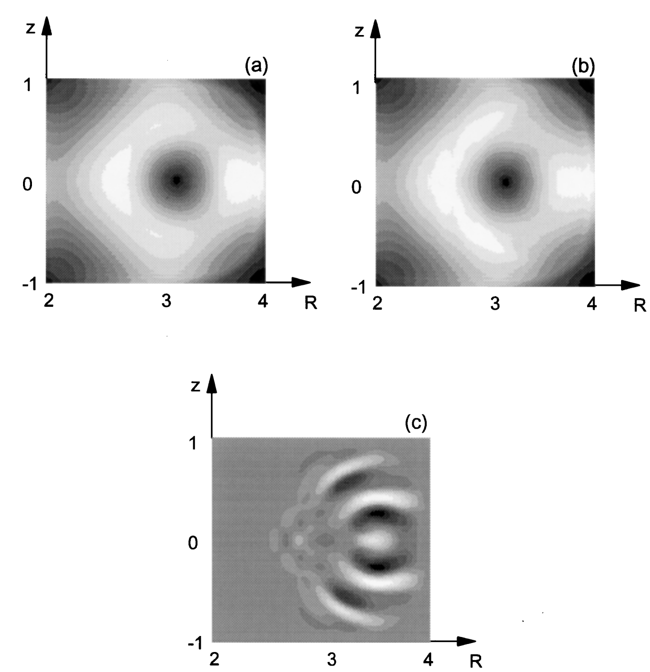

FIG. 2. Temporal evolution of the magnitude of the poloidal magnetic field in the poloidal plane at $\phi = 0$, at $t/\tau_A = 0$ (a) and 180 (b). The momentum in the direction of the major radius at $t = 180\tau_A$ is plotted in (c).

rises as n increases beyond unity, peaking at $n = 6$. For larger $n > 6$, the growth rate continuously decreases as n increases. The effect on γ of lowering $\eta = \mu$ varies depending on the toroidal mode number. When n is small, the growth rate decreases as $\eta = \mu$ decreases. However, for larger n the opposite is true; the growth rate increases as $\eta = \mu$ decreases. Overall, as $\eta = \mu$ decreases there is an increase in the peak growth rate in the spectrum and a shift to larger n of the fastest growing mode. Thus, the rapid loss of confinement seen in the nonlinear simulation in Fig. 1 is not caused by the use of a relatively large $\eta = \mu$. To the contrary, from Fig. 3 one would expect that, as $\eta = \mu$ decreases, confinement would be destroyed even a little more rapidly. We have demonstrated this by repeating the nonlinear simulation with a reduced value of $\eta = \mu = 2 \times 10^{-4}$. The result is shown in Fig. 4. This figure is a plot of the pressure in the poloidal plane at $t = 180\tau_A$ after the application of the perturbation when $\eta = \mu = 2 \times 10^{-4}$, and is to be compared with Fig. 1(d) where $\eta = \mu$ is 50% larger. The results in the two cases are nearly the same. The maximum value of the poloidal velocity, denoted by $v_{\max}$, is a measure of the rate at which confinement is destroyed by the cross field convection of energy. During the simulation shown in Fig. 1, $v_{\max}$ increases continuously in time from a small perturbation to a large value as confinement is lost. At $t = 180\tau_A, v_{\max}/v_A = 7.1 \times 10^{-3}$, when $\eta = \mu = 2 \times 10^{-4}$, while $v_{\max}/v_A = 6.6 \times 10^{-3}$, when $\eta = \mu = 3 \times 10^{-4}$. Thus, there is actually a small 8% increase in the rate at which confinement is destroyed (not a decrease) for a 33% decrease in $\eta = \mu$. The viscosity tends to damp the convective motion of the plasma across the magnetic field. When μ is reduced, the growth rate of the extended convective vortices increases.

Alteration of the current profile has no appreciable effect on the loss of thermal confinement in the nonlinear simulation. When the central safety factor q_0 is reduced from 1.1 to 0.9, confinement is destroyed in exactly the same manner as shown in Fig. 1, and at the same rate. Thus, the presence of a $q = 1$ surface, or lack thereof, in the plasma has no effect on the loss of confinement. When the parameter l is lowered from $l = 2$ to $l = 1$, the shear in the magnetic field around the magnetic axis is increased. But confinement is still destroyed by fingers of hot and cold plasma whose growth does not saturate on the same time scale as in the lower central shear $l = 2$ case. The pressure profile used in the simulation shown in Fig. 1 is flat around the magnetic axis, with $dP/d\psi = 0$ at the axis. Confinement in a $\beta_{\text{pol}} = 1$ equilibrium with a more peaked pressure profile given by $P(\psi) = P_0(\psi/\psi_0)^2$, with $dP/d\psi \neq 0$ at the magnetic axis, is destroyed in an analogous manner on the same time scale.

The results in Figs. 1 and 2 demonstrate that fingers of hot and cold plasma rapidly jet across magnetic field lines during the nonlinear evolution of MHD instabilities in high β tokamaks. The rapid motion of particles along the magnetic field lines, physics not included in the MHD approximation, acts both to transport energy from the hot fingers to the cold fingers and to diffuse the hot plasma from the bad curvature (outside) region to the good curvature (inside) region, thereby reducing the drive for the instability. In order to ascertain the impact of parallel transport on the growth of the fingers, we have included the physics of parallel heat transport in our MHD simulations. For the TFTR disruption parameters discussed previously, the electron-ion collision time $\tau_{\text{ei}} \approx 250\ \mu$sec while the ion-ion collision time τ_{ii} is longer still by the square root of the ratio of the ion mass M_i to the electron mass m_e. Thus, the collision time is much longer than the time scale over which energy is lost during β limit disruptions. As a consequence, during the short disruption time scale the plasma is collisionless, and energy is transported along the field lines by free-streaming particles. Since the plasma is collisionless, the only coupling between electrons and ions occurs because of electric fields created by charge separation, and the electrons are forced to follow the ions because the ions are much more massive. The rate of free-streaming transport of ion energy along the magnetic field lines is unaffected by the much less massive electrons. To model the free-streaming ion transport in our simulations, we include a term $-\nabla_{\|}\kappa_{\|}(t)\nabla_{\|}T$ in the equation for the time rate of change of the pressure P, where the temperature $T = P/\rho_m$, and $\nabla_{\|}$ is the parallel gradient along the magnetic field. With a time-dependent parallel thermal coefficient $\kappa_{\|} = v_i^2 t$, where v_i is the ion thermal speed, the time scale $\tau_{\|}$ for the transport of energy a distance s down a magnetic field line is given by the free-streaming result $\tau_{\|} = s/v_i$. For times t longer than a collision time $\tau_{\text{ii}}, \kappa_{\|}(t) \to \kappa_{\|}(\tau_{\text{ii}}) = v_i^2 \tau_{\text{ii}}$, the collisional result. The effect of collisionless parallel energy transport on the MHD stability of the $\beta_{\text{pol}} = 1$ equilibrium is shown in Fig. 5. This figure is a plot of the pressure at $t = 210\tau_A$ after the application of the perturbation shown in Fig. 1(a). Confinement has been destroyed in the same manner as that shown in Fig. 1. This simulation demonstrates that collisionless parallel transport is not rapid enough to prevent the loss of thermal confinement. The reason for the ineffectiveness of parallel transport can be seen by

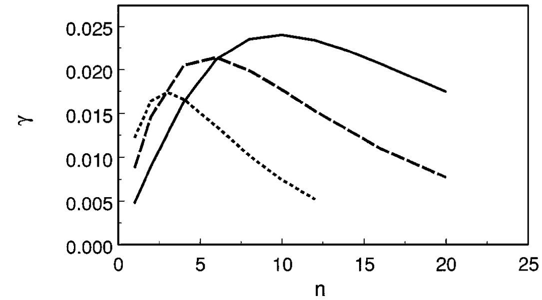

FIG. 3. Linear stability. The growth rate γ, normalized to the Alfvén time τ_A, is plotted for modes with toroidal mode number n, for three different values of the resistivity: $\eta = \mu = 1 \times 10^{-3}$ (dotted line); 3×10^{-4} (dashed line); 1×10^{-4} (solid line).

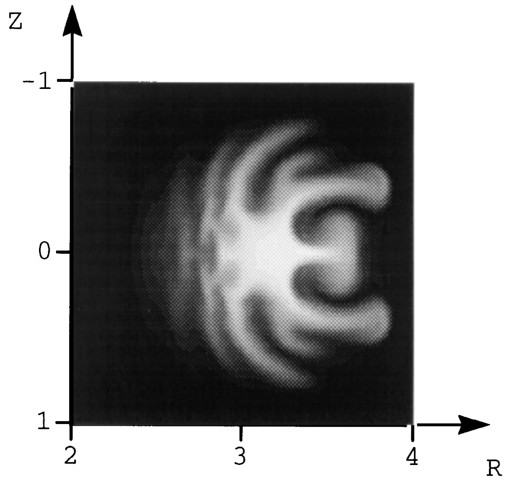

FIG. 4. Pressure in the poloidal plane (R, z) at $\phi = 0$ for a plasma with $\beta_{\text{pol}} = 1.0$ and $\eta = \mu = 2 \times 10^{-4}$, at $t/\tau_A = 180$.

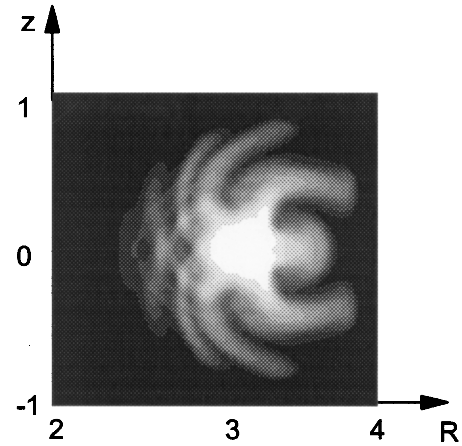

FIG. 5. Parallel thermal transport. The pressure in the poloidal plane at $t/\tau_A = 210$ is plotted for a plasma with the same parameters as those in Fig. 1, but with a parallel energy transport coefficient $\kappa_{\parallel} = v_i^2 t$.

calculating the distance a thermal ion travels down a field line in a short MHD growth time. The peak ion thermal velocity in the $\beta_{\text{pol}} = 1$ equilibrium is $v_{i,\max}/v_A = 8 \times 10^{-2}$. From Fig. 3, the growth time τ_{MHD} of the fastest growing $n = 6$ mode is $\tau_{\text{MHD}} = 47\tau_A$. Therefore, the distance $s = v_{i,\max}\tau_{\text{MHD}}$ traveled by an ion in a growth time τ_{MHD} is $s/2\pi R_0 = 0.2$, only about one-fifth of the way around the torus. The cross field loss of confinement in high β plasmas is so rapid that even collisionless, free-streaming ion motion along the undisturbed magnetic field lines is not fast enough to counteract it.

The results in this Letter contradict the conclusions drawn in Ref. [3]. There it is claimed that the thermal quench is caused by transport along stochastic magnetic field lines, resulting from the destruction of magnetic flux surfaces. But the diffusion of energy along stochastic magnetic field lines is much too slow a process to account for the rapid loss of confinement in high β disruptions, unless the magnitude of the stochastic magnetic field is extremely large, much larger than is observed experimentally. We can estimate the magnitude of the stochastic magnetic field required to rapidly destroy confinement from the collisionless diffusion coefficient [4–6] $D_{\tilde{B}} = (\tilde{B}/B_\phi)^2 L_s v_i$ for transport in a stochastic magnetic field of magnitude $\tilde{B}$, where B_ϕ is the toroidal magnetic field, and L_s is the shear length of the equilibrium magnetic field. For the TFTR parameters discussed previously, and for $L_s \approx R_0$, we find that the stochastic magnetic field required to diffuse energy across the minor radius in 20 μsec is very large: $\tilde{B}/B_\phi \approx 0.12$, which yields $\tilde{B} \approx 5$ kG. This stochastic magnetic field is as large, or larger, than the magnitude of the poloidal magnetic field across the entire cross section. This result is in disagreement with experimental observations of β limit disruptions on TFTR [1], where there is no evidence of flux reconnection or large magnetic perturbations. The equations used in Ref. [3] include terms that model the transport of energy along magnetic field lines as a wave propagation at the electron thermal velocity. But free-streaming ions transport their energy down the magnetic field lines at the much slower ion thermal velocity.

In summary, our MHD simulations demonstrate that confinement in high β tokamaks is destroyed by fingers of hot plasma which jet out from the center of the discharge to the edge, while fingers of cold edge plasma are injected into the center. This loss of confinement is extremely fast; confinement is destroyed in just a few tens of microseconds, in agreement with experimental observations. The magnetic field is virtually unchanged during the rapid loss of thermal confinement, which is also in agreement with experimental observations. The cross field loss of energy is so fast that even the free-streaming motion of ions along the undisturbed magnetic field lines is not rapid enough to counteract it. The stabilizing effect of parallel transport on more slowly growing MHD modes at lower β will be discussed in a future publication. The impact of electron inertia (nonideal MHD) on these rapidly growing modes is a subject for future research.

[1] E.R. Fredrickson, K. McGuire, Z. Chang, A. Janos, M. Bell, R.V. Budny, C.E. Bush, J. Manickam, H. Mynick, R. Nazikian, and G. Taylor, Phys. Plasmas **2**, 4216 (1995).
[2] R.G. Kleva, Phys. Plasmas **3**, 2337 (1996).
[3] W. Park, E.D. Fredrickson, A. Janos, J. Manickam, and W.M. Tang, Phys. Rev. Lett. **75**, 1763 (1995).
[4] J.R. Jokipii and E.N. Parker, Astrophys. J. **155**, 777 (1969).
[5] A.B. Rechester and M.N. Rosenbluth, Phys. Rev. Lett. **40**, 38 (1978).
[6] J.A. Krommes, C. Oberman, and R.G. Kleva, J. Plasma Phys. **30**, 11 (1983).